




# TIDE: Achieving Balanced Subject-Driven Image Generation via Target-Instructed Diffusion Enhancement

Jibai Lin<sup>1,2,3</sup>  Bo Ma<sup>1,2,3</sup>  Yating Yang<sup>1,2,3</sup>  Rong Ma<sup>1,2,3</sup> Turghun Osman<sup>1,2,3</sup> Ahtamjan Ahmat<sup>1,2,3</sup>  
Rui Dong<sup>1,2,3</sup> Lei Wang<sup>1,2,3</sup> Xi Zhou<sup>1,2,3</sup>

<sup>1</sup>Xinjiang Technical Institute of Physics & Chemistry, Chinese Academy of Sciences

<sup>2</sup>University of Chinese Academy of Sciences

<sup>3</sup>Xinjiang Laboratory of Minority Speech and Language Information Processing

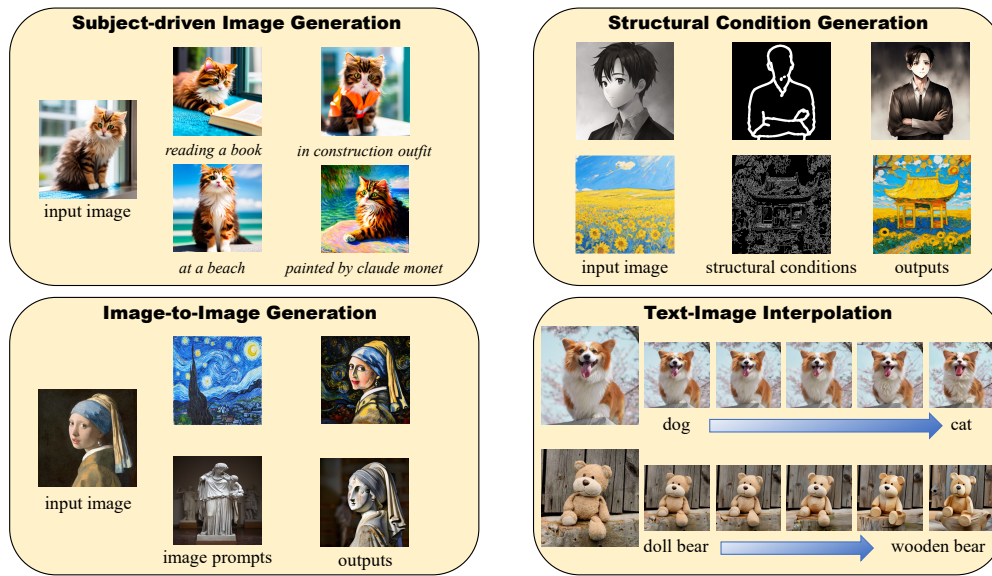


Figure 1: Our TIDE framework achieves high-fidelity subject-driven generation from single reference images via target-supervised learning. Our model also supports diverse tasks like structure-controlled generation, image-to-image generation, and interpolation between reference images and textual prompts to demonstrate its versatility in subject manipulation.

## Abstract

*Subject-driven image generation (SDIG) aims to manipulate specific subjects within images while adhering to textual instructions, a task crucial for advancing text-to-image diffusion models. SDIG requires reconciling the tension between maintaining subject identity and complying with dynamic edit instructions, a challenge inadequately addressed by existing methods. In this paper, we introduce the Target-Instructed Diffusion Enhancing (TIDE) framework, which resolves this tension through target supervision and preference learning without test-time fine-tuning. TIDE pioneers target-supervised triplet alignment, modelling subject adaptation dynamics using a (reference image, instruction, target images) triplet. This approach leverages the Direct Subject Diffusion (DSD) objective, training the model with paired "winning" (balanced preservation-compliance) and "losing" (distorted) targets, systematically generated and evaluated via quantitative metrics. This enables implicit reward modelling for optimal preservation-compliance balance. Experimental results on standard benchmarks demonstrate TIDE's superior performance in generating subject-faithful outputs while maintaining instruction compliance, outperforming baseline methods across multiple quantitative metrics. TIDE's versatility is further evidenced by its successful application to diverse tasks, including structural-conditioned generation, image-to-image generation, and text-image interpolation. Our code is available at <https://github.com/KomJay520/TIDE>.*

**Keywords:** Subject-driven image generation, Diffusion models, Target supervision, Preference learning, Triplet alignment

## 1. Introduction

Subject-Driven image generation (SDIG) aims to synthesize images that preserve the identity of a specified subject (e.g., a cat, object) while adapting to textual editing instructions (e.g., "The cat\* swimming in a pool") [Gal et al.(2022), Ruiz et al.(2023), Kumari et al.(2023), Li et al.(2023), Zhang et al.(2024)]. This task extends text-to-image diffusion models [Dhariwal and Nichol(2021), Rombach et al.(2022), Ahn et al.(2024), Chefer et al.(2024)] to enable controlled subject manipulation, critically expanding their utility for realistic applications like personalized content creation and visual storytelling. At its core, SDIG demands precise reconciliation of two competing objectives: invariant preservation of subject identity against dynamic compliance with edit instructions. This process advances controllable generation techniques for real-world subject editing scenarios.

Existing SDIG methods can be broadly classified into fine-tuning based and fine-tuning free methods, with the key distinction lying in whether they perform parameter updates during test time. On the one hand, fine-tuning based methods fine-tune pre-trained diffusion model or its components using 3-5 reference images at test-time [Ruiz et al.(2023), Avrahami et al.(2023), Hyung et al.(2024)]. These methods embed subject features into a placeholder token (e.g., [V]) and combine it with text prompts (e.g., The [V] cat swimming in a pool) to generate subject-driven images. However, they suffer from catastrophic forgetting: retraining on novel subjects leads to the overwriting of previously learned representations limiting their scalability to diverse subject domains. On the other hand, fine-tuning free methods preserve parameters of base model by encoding reference images via external modules (CLIP/BLIP) and injecting subject features through trainable adapters [Li et al.(2023), Zhang et al.(2024), Ma et al.(2024)]. Yet, their self-supervised reconstruction paradigm, as shown in the top row of Figure 2, is forced to use reference images as pseudo-targets. Due to missing instruction-edited pairs, they conflate preservation (e.g., retaining object appearance) and modification (e.g., altering background). This ambiguity prevents models from learning the critical balance between feature retention and semantic adaptation. In summary, existing approaches fail to inadequate balance subject preservation and instruction compliance: fine-tuning based methods sacrifice generalization for subject fidelity, while fine-tuning free methods lack explicit supervision for edit disentanglement.

To resolve the preservation-compliance trade-off, we propose TIDE (Target-Instructed Diffusion Enhancing), a fine-tuning-free framework built upon two key innovations: explicit triplet supervision and the Direct Subject Diffusion (DSD) objective. First, as demonstrated in the middle row of Figure 2, TIDE introduces reference-instruction-target triplet supervision, which is a structured guidance mechanism absent in prior self-supervised methods. Unlike approaches that rely solely on reference images as targets (top row), the target images in triplet explicitly encode desired attribute edits (e.g., pose, background changes), enabling the model to learn fine-grained mappings between instructions and subject adaptations. Crucially, TIDE proposes the DSD objective tailored for SDIG. Specifically, DSD adapts the pairwise preference learning to image generation by integrating subject-specific features from reference images, enabling the model to learn from

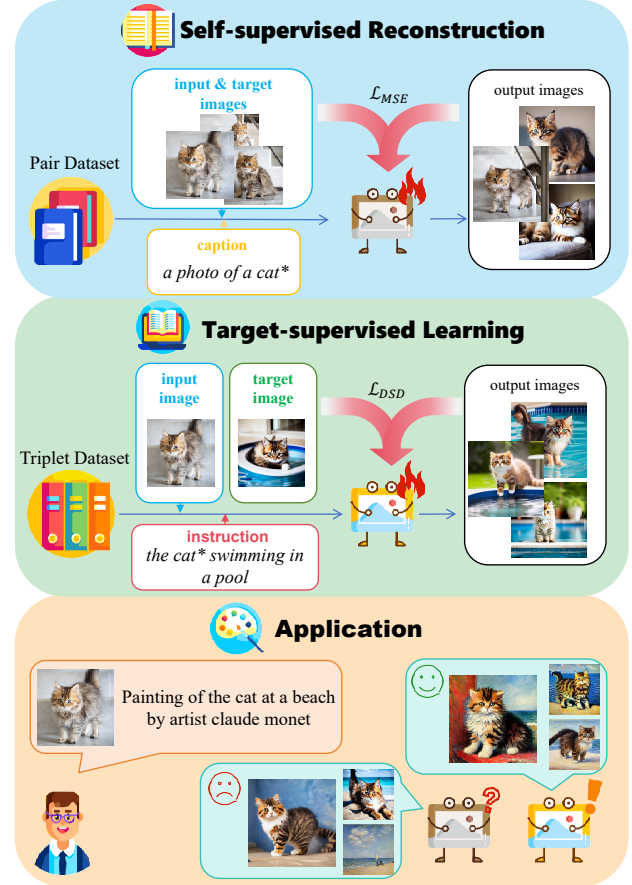


Figure 2: Different of Self-supervised Reconstruction and Target-supervised Learning in subject-driven image generalization. Self-supervised Reconstruction always use the input images as label images, result to bad output in applications.

paired "winning"/"losing" target images. For each instruction (e.g., "Cat swimming in a pool"), the preference pairs which encode human-like quality judgments for balanced outputs, train the model to prefer "winning" targets (balanced outputs) over "losing" targets (unbalanced, e.g., instruction or feature loss). This preference signal allows TIDE to implicitly model a reward function that guides the diffusion process to generate semantically consistent images while preserving critical subject attributes. As visualized in Figure 2 bottom-row comparisons, TIDE generates images faithfully following instructions while preserving subject identity.

To implement these innovations, we adapt prior multimodal fusion techniques through an Image Projection Module with Image Cross-Attention Module (IPM-ICAM). This module encodes reference features to condition the diffusion process. Extensive experiments have shown that our method with this lightweight module achieves comparable results to other methods in subject-driven image generation.

To summarize, our contributions are listed as follows:

- We propose a novel framework, named TIDE, for personalized



subject-driven image generation, which uses triplet data to explicitly specify feature preservation and modification rules.

- In TIDE, we propose Direct Subject Diffusion, a novel preference learning objective that enables implicit optimization of both subject fidelity and instruction compliance.
- Our extensive experiments have validated the robustness and flexibility of our approach, showcasing its capability to deliver competitive performance among SDIG methods. It also supports diverse tasks including structural-conditioned generation, image-to-image generation, and text-image interpolation.

## 2. Related Work

### 2.1. Aligning Large Language Models

LLMs [Achiam et al.(2023), Ye et al.(2024)] are typically aligned with human preferences through supervised fine-tuning (SFT) [Dong et al.(2023)] on demonstration data followed by reinforcement learning from human feedback (RLHF) [Bai et al.(2022)]. RLHF learns a reward model from pairwise output comparisons to guide policy optimization via policy-gradient methods [Mnih et al.(2016)], but faces notable challenges including high computational costs from nested training loops, sensitivity to hyperparameter choices, and susceptibility to reward hacking [Dubois et al.(2023), Skalse et al.(2022)]. Recent approaches mitigate these issues through reward-weighted supervised learning, ranking loss minimization and direct policy optimization [Krishnaiah et al.(2024), Rafailov et al.(2023), Dubois et al.(2023)]. The latter matches the performance of RLHF without its complexity. Direct Preference Optimization (DPO) has since been widely adopted to bridge structural discrepancies in various domains. Inspired by DPO [Rafailov et al.(2023), Wallace et al.(2024)], a framework that transforms RLHF into a supervised learning problem, our method leverages its core principles to address subject-driven alignment challenges. Promising extensions using AI feedback [Bai et al.(2022)] suggest pathways for scalable alignment in SDIG.

### 2.2. Text-to-image models

Recent advancements in large-scale diffusion models have significantly expanded their applicability in image synthesis [Ramesh et al.(2021), Ramesh et al.(2022), Rombach et al.(2022), Podell et al.(2023), Lin et al.(2024)]. Among these, latent diffusion models (LDMs) [Rombach et al.(2022)] have emerged particularly noteworthy due to their computational efficiency. The evolution of text-to-image generation began with DALL-E [Ramesh et al.(2021)] which introduces the autoregressive transformer architecture, followed by innovative integration of a diffusion prior module with cascaded super-resolution decoders in DALL-E-2 [Ramesh et al.(2022)]. Concurrently, Imagen [Saharia et al.(2022)] demonstrated the effectiveness of large pretrained language models (T5) [Raffel et al.(2020)] for enhanced textual understanding combined with large-scale diffusion training. DeepFloyd IF [Saharia et al.(2022)] further advanced the field through a three-stage cascaded diffusion architecture capable of generating legible typography. Stable Diffusion (SD) [Rombach et al.(2022)] established itself as a benchmark by introducing cross-attention mechanisms for precise text-conditioned generation, combining high-quality output

with computational practicality. Our framework builds upon Stable Diffusion, selected for its modular design and open-source availability, features that facilitate extensible adaptation.

### 2.3. Subject-driven Diffusion models

The widespread adoption of diffusion models for text-to-image synthesis has naturally extended to subject-driven generation tasks [Gal et al.(2022), Ruiz et al.(2023), Wei et al.(2023), Ye et al.(2023), Li et al.(2023), Zhang et al.(2024), Ma et al.(2024)]. There are two main frameworks for customized subject-driven image generation from the perspective of whether to introduce test-time fine-tuning.

Fine-tuning based methods often optimize additional text embeddings or directly fine-tune the diffusion model to fit the desired subject [Gal et al.(2022), Ruiz et al.(2023), Kumari et al.(2023)]. For instance, Textual Inversion [Gal et al.(2022)] aligns subject image with additional text embeddings, while DreamBooth [Ruiz et al.(2023)] adjusts the entire U-net in the diffusion model. Other methods like Custom Diffusion [Kumari et al.(2023)] and Cones [Liu et al.(2023a)] only fine-tune the K and V layers of the cross-attention. SVDiff [Han et al.(2023)] fine-tunes the singular values of the weight matrices. These methods both try to minimize the parameters needing finetuning and reduce computational demands. On the other hand, after Custom Diffusion [Kumari et al.(2023)] proposes the personalized generation of multiple subjects for the first time, Cones2 [Liu et al.(2023b)] generates two-subject combination images by learning the residual of token embedding and controlling the attention map. MagiCapture [Hyung et al.(2024)] introduces a multi-concept personalizing method capable of generating high-resolution portrait images that faithfully capture the characteristics of both source and reference images. Perfusion [Tewel et al.(2023)] develop a gated rank-1 approach that enables us to control the influence of a learned concept during inference time and to combine multiple concepts.

Although fine-tuning based methods have better subject guidance ability, they suffer from a catastrophic forgetting problem and ineffective usage problem (e.g., given a new subject, these methods require complete model retraining, leading to efficiency bottlenecks), another research route involves constructing a large amount of domain-specific data or using open-domain image data for training without additional fine-tuning. Fine-tuning-free methods typically train an additional structure to encode the reference image into embeddings or image prompts [Gal et al.(2023), Ye et al.(2023), Ma et al.(2024)]. E4T [Gal et al.(2023)] uses a set of weight-offsets for the text-to-image model that learn how to effectively ingest additional concepts. ELITE [Wei et al.(2023)] employs global and local mapping trained on OpenImages [Kuznetsova et al.(2020)], but achieves limited text alignment due to architectural constraints. InstantBooth [Shi et al.(2024)] proposes an adapter structure inserted in the U-net. UMM-Diffusion [Ma et al.(2023)] introduces a novel Unified Multi-Modal Latent Diffusion that processes joint text-image inputs containing target subjects to generate customized outputs. However, its reliance on the LAION-400M [Schuhmann et al.(2021)] dataset limits performance for rare themes. Similarly, domain-specific training data is employed by E4T, InstantBooth, FastComposer [Xiao et al.(2024)], and Face-Diffuser [Wang et al.(2024)]. BLIP-

Diffusion [Li et al.(2023)] propose two-stage training scheme to achieve good fidelity effects. IP-Adapter [Ye et al.(2023)] encodes images into prompts with a lightweight adapter and decoupled cross-attention strategy. Subject-Diffusion [Ma et al.(2024)], SSR-Encoder [Zhang et al.(2024)] and FreeCustom [Ding et al.(2024)] use segmentation network to mask the key concept from visual input, improving subject consistency in multi-subjects-driven generation. These methods still rely on self-supervised reconstruction objectives, resulting in failure to maintain subject consistency under complex editing instructions. Specifically, this limitation stems from their training paradigm, which uses input images as reconstruction targets and captions as proxy instructions, ultimately limiting their adaptability to diverse editing commands. These critical limitations motivate our work's key innovations.

### 3. Preliminaries

#### 3.1. Diffusion Models

Diffusion models (DMs) learn to generate samples by progressively denoising a Gaussian-distributed variable, starting from data samples drawn from the distribution  $q(x_0)$ . They are trained to reverse diffusion processes that reconstruct clean data from noisy inputs. The forward diffusion process is defined as:

$$x_t = \sqrt{1 - \beta_t}x_{t-1} + \sqrt{\beta_t}n_t, \quad t = 1, \dots, T \quad (1)$$

where  $x_0$  is the source image from dataset,  $\beta_t$  denotes the noise schedule and  $n_t$  represents independent and identically distributed (i.i.d.) Gaussian noise vectors. Through mathematical derivation, the process can be equivalently expressed as:

$$x_t = \sqrt{\bar{\alpha}_t}x_0 + \sqrt{1 - \bar{\alpha}_t}\epsilon_t \quad (2)$$

where  $\alpha_t = 1 - \beta_t$ ,  $\bar{\alpha}_t = \prod_{i=1}^t \alpha_i$  and  $\epsilon_t \sim \mathcal{N}(0, I)$  is random Gaussian noise. We use this algorithm to inverse our target images. Then to generate a new image  $\hat{x}_0$  following the deterministic DDIM [Song et al.(2020)], the reverse diffusion process starts from a random noise  $\hat{x}_T \sim \mathcal{N}(0, I)$ , which can be iteratively denoised as:

$$\begin{aligned} \hat{x}_{t-1} = & \sqrt{\bar{\alpha}_{t-1}} \frac{\hat{x}_t - \sqrt{1 - \bar{\alpha}_t} \epsilon_\theta(\hat{x}_t)}{\sqrt{\bar{\alpha}_t}} \\ & + \sqrt{1 - \bar{\alpha}_{t-1}} \epsilon_\theta(\hat{x}_t), \quad t = T, \dots, 1 \end{aligned} \quad (3)$$

Here  $\epsilon_\theta(\cdot)$  is an estimate of  $\epsilon_t$  produced by our frozen neural network DM and a trainable adapter model with learned parameters  $\theta$ . For SDIG, the model is conditioned on a text prompt  $p$  and subject images  $I$  to produce images faithful to these. Instead of estimating the loss between image outputs and target outputs, DMs' training is performed by minimizing the evidence lower bound (ELBO) [Kingma et al.(2021)]:

$$L_{DM} = \mathbb{E}_{\hat{x}_0, \epsilon, t, \hat{x}_t} \left[ \omega(\lambda_t) \|\epsilon - \epsilon_\theta(\hat{x}_t, c_p, t)\|_2^2 \right] \quad (4)$$

where  $\lambda_t$  is a signal-to-noise ratio,  $\omega(\lambda_t)$  is a pre-specified weighting function which typically keeps constant, timestep  $t \sim \mathcal{U}(0, T)$ ,  $c_p$  is the condition (or feature) from  $p$ .

#### 3.2. DPO for Diffusion Models

RLHF aims to optimize a conditional distribution  $p_\theta(y_0|c)$  (conditioned on  $c \sim \mathcal{D}_c$ ,  $y_0$  is target output) such that the latent reward

model  $r(c, y_0)$  define on it is maximized, while regularizing the KL-divergence from a reference distribution  $p_{ref}$ :

$$\begin{aligned} \max_{p_\theta} \mathbb{E}_{c \sim \mathcal{D}_c, y_0 \sim p_\theta(y_0|c)} [r(c, y_0)] \\ - \beta \mathbb{D}_{KL}[p_\theta(y_0|c) || p_{ref}(y_0|c)] \end{aligned} \quad (5)$$

where the hyperparameter  $\beta$  controls regularization.

In DPO [Rafailov et al.(2023)], we always assume access only to ranked pairs generated from some conditioning  $y_0^w \succ y_0^l|c$ , where  $y_0^w$  and  $y_0^l$  denote the "winning" (positive) and "losing" (negative) samples. With the loss function of Bradley-Terry (BT) model [Imrey(2005)], the loss function is estimated via maximum likelihood training for binary classification:

$$L_{BT}(\phi) = -\mathbb{E}_{c, y_0^w, y_0^l} [\log \sigma(r_\phi(c, y_0^w) - r_\phi(c, y_0^l))] \quad (6)$$

where  $\sigma$  is the sigmoid function.  $r_\phi(\cdot)$  is reward function which is parameterized by a neural network  $\phi$ . Using Eq.(5), this leads to the DPO objective:

$$L_{DPO}(\theta) = -\mathbb{E}_{c, y_0^w, y_0^l} \left[ \log \sigma \left( \beta \log \frac{p_\theta(y_0^w|c)}{p_{ref}(y_0^w|c)} - \beta \log \frac{p_\theta(y_0^l|c)}{p_{ref}(y_0^l|c)} \right) \right] \quad (7)$$

By combining Eq.(4) and Eq.(7), DPO-Diffusion (DD) [Wallace et al.(2024)] adapt DPO for diffusion model yields:

$$\begin{aligned} L_{DD}(\theta) = & -\mathbb{E}_{(p, y_0^w, y_0^l) \sim \mathcal{D}, t \sim \mathcal{U}(0, T), y_t^w \sim q(y_t^w | y_0^w), y_t^l \sim q(y_t^l | y_0^l)} \\ & \log \sigma(-\beta T \omega(\lambda_t) ( \\ & \|\epsilon^w - \epsilon_\theta(y_t^w, c_p, t)\|_2^2 - \|\epsilon^w - \epsilon_{ref}(y_t^w, c_p, t)\|_2^2 \\ & - (\|\epsilon^l - \epsilon_\theta(y_t^l, c_p, t)\|_2^2 - \|\epsilon^l - \epsilon_{ref}(y_t^l, c_p, t)\|_2^2))) \end{aligned} \quad (8)$$

where  $q(y_t^w | y_0^w)$  is the diffusion process following Eq.(2),  $\epsilon_{ref}(\cdot)$  denotes predictions from the frozen reference model.

### 4. Methodology

In this section, we first present our open-domain instruction-target dataset for supervised training in SDIG. Next, we show an overview of the TIDE framework, followed by an explanation of how we leverage multimodal information to train external adapter, including multimodal representation and Direct Subject Diffusion optimization.

#### 4.1. Dataset Construction

To enable diffusion models to balance subject preservation and instruction compliance, a multimodal supervised dataset with open-domain coverage is essential. Existing datasets [Kuznetsova et al.(2020), Schuhmann et al.(2022)], primarily designed for multimodal alignment and visual question answering (e.g., image-caption pairs), prove inadequate for this purpose due to their inherent structural limitations. This motivates our creation of a tailored, high-quality dataset comprising three core components: (1) visual subject inputs, (2) structured textual instructions with fine-grained control parameters, and (3) corresponding target outputs optimized for subject-driven generation scenarios.

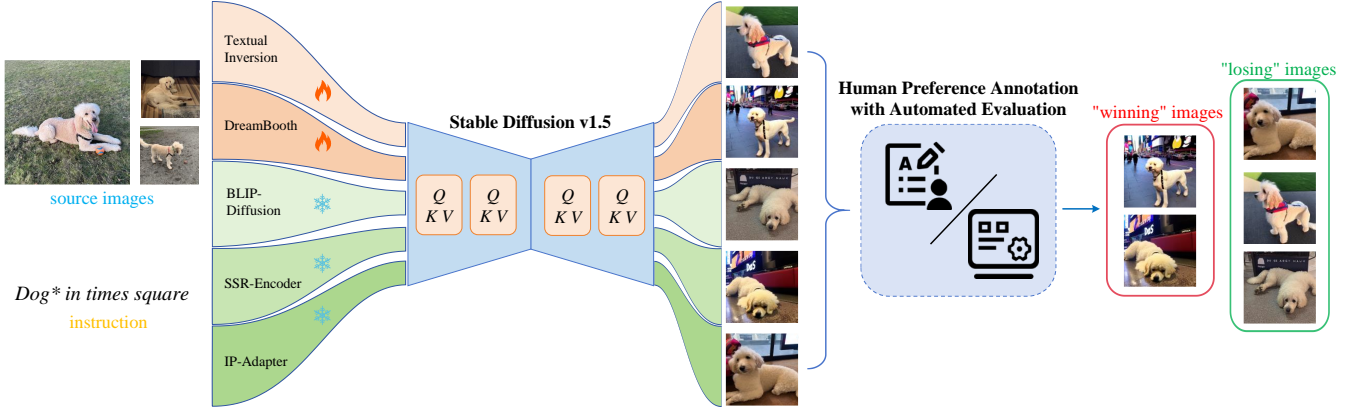


Figure 3: The procedure for training data generation. (i) Samples are first generated using different baseline methods with the same diffusion model. Among them, Textual Inversion and DreamBooth require fine-tuning the model, while others do not. (ii) Using automated evaluation models (CLIP, DINO), generated samples are sorted: level 5-4 samples are selected as "winning" samples, and the rest as "losing" samples.

Figure 3 illustrates our methodology for constructing the training dataset derived from Concept101 [Kumari et al. (2023)] benchmark, which provides diverse and semantically rich instructions per subject. We employ existing subject-driven image generation techniques to produce candidate outputs, and then use quantifiable quality metrics, the similarity of CLIP and DINOv2 embeddings, to select "winning" and "losing" sample pairs. Specifically, we calculate the similarity between the embeddings of the output samples and prompts. We use a hyperparameter  $\phi$  to balance the textual similarity and the visual similarity. For each candidate output, we compute two normalized similarity metrics: (1)  $S_{text} = \text{mean}(\text{CLIP}(x_p) \cdot \text{CLIP}(y_0)^\top)$  for instruction alignment, and (2)  $S_{visual} = \cos(\text{DINO}(x_i), \text{DINO}(y_0))$  for subject alignment. The composite quality score  $Q$  is then computed as:

$$Q = \phi \cdot S_{text} + (1 - \phi) \cdot S_{visual} \quad (9)$$

where  $\phi \in [0, 1]$  is a tunable hyperparameter that balances the relative importance of textual versus visual fidelity. Through extensive grid search, we set  $\phi = 0.7$  to prioritize instruction following while maintaining adequate subject preservation.

Through this automated selection strategy, we establish C4DD (Concept101 for DPO Dataset). Image candidates are ranked into five quality levels (Level 5: highest  $Q$ ), where Level 5-4 images are designated as "winning" samples and Level 3-1 as "losing" samples (Figure 4). This dataset contains 10,000 high-quality samples with 6,000 carefully curated (winning, losing) pairs. To the best of our knowledge, C4DD is the first target-supervised dataset for SDIG.

#### 4.2. Model Overview

As illustrated in Figure 5, TIDE framework resolves the preservation-compliance trade-off through three coordinated design principles. First, the input pipeline processes triplets of instruction  $x_p$ , source image  $x_i$  and "winning"/"losing" target images  $(y_0^w, y_0^l)$  from our C4DD. The target images establish explicit supervision for balanced generation. Second, the trainable adapter IPM-

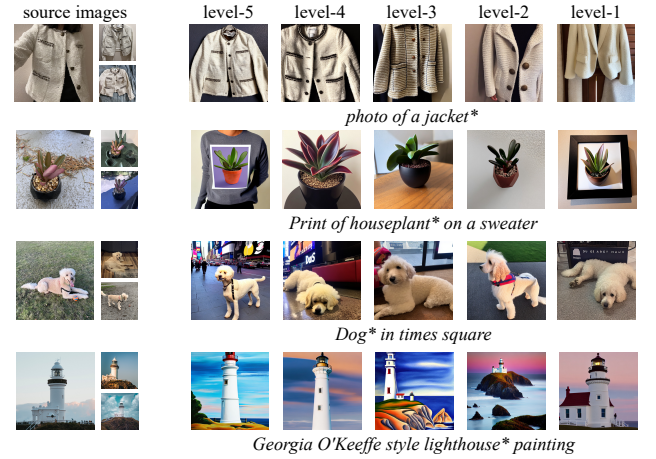


Figure 4: Sample images from the dataset showing source and target images with instructions. Level 5 means the best target image. We choose the level 5-4 images as the winning samples.

ICAM dynamically align source image feature  $c_i$  with instruction feature  $c_p$ . And then the diffusion model predict the noise relying on this multimodal feature  $F(c_p, c_i)$ . Third, by leveraging the DDIM forward diffusion following the Eq. (2), we get the noise signals  $\epsilon^w$  and  $\epsilon^l$  from the target images. The DSD objective can operate in noise space by comparing predictions of  $\epsilon^w$  and  $\epsilon^l$ . The loss optimizes the trainable adapter to concentrate on gaps between "winning" and "losing" targets through preference-aware gradients.

#### 4.3. Multimodal Representation

Our framework builds on the native architecture of Stable Diffusion, which employs a frozen CLIP text encoder for prompt conditioning. To ensure modality consistency, we adopt the CLIP image encoder for subject representation extraction, leveraging their

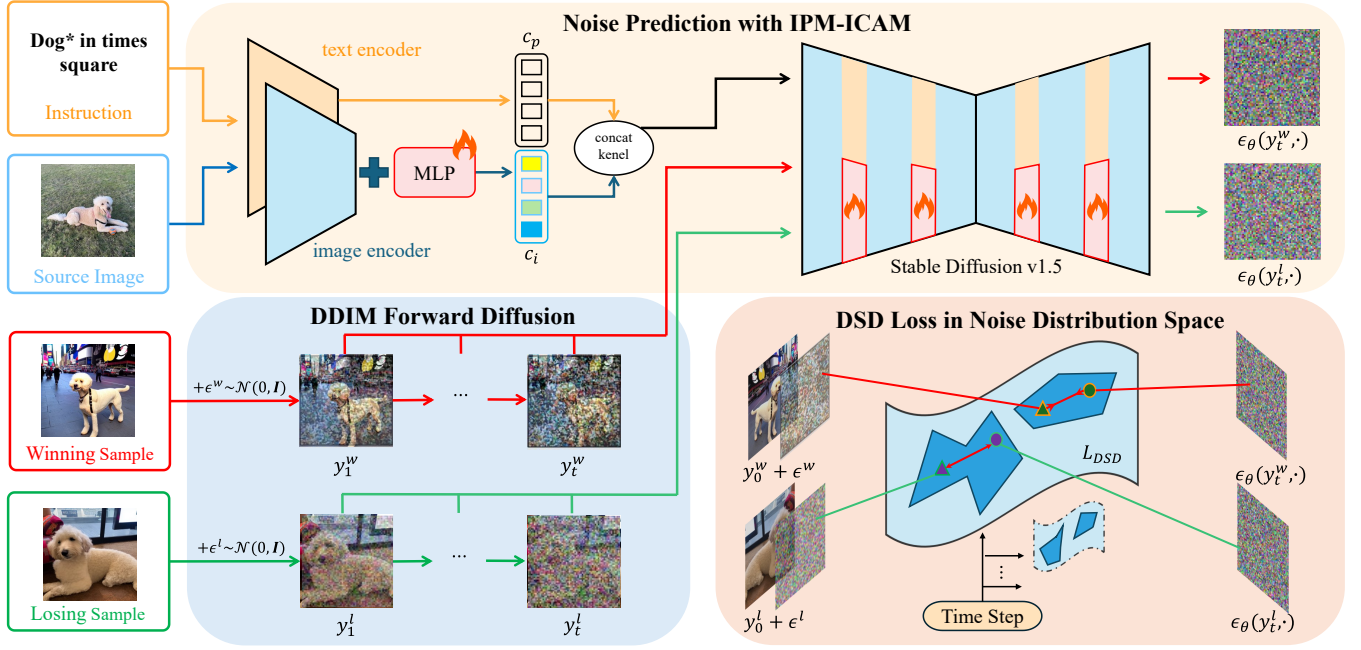


Figure 5: Illustration of the DSD training for TIDE. (i) Given a query instruction-image pair, we first design IPM-ICAM to align the image feature  $c_i$  with instruction embedding  $c_p$ . (ii) Then, based on DDIM forward diffusion, we convert target samples into noisy latent ( $y_t^w, y_t^l$ ) and their noise residuals ( $\epsilon^w, \epsilon^l$ ) at timestep  $t$ . (iii) After that, Stable Diffusion v1.5 predicts the target noise from noisy latent using fused multimodal feature  $F(c_p, c_i)$ . (iv) Finally, the DSD loss compares predicted noise ( $\epsilon_\theta(y_t^w, \cdot), \epsilon_\theta(y_t^l, \cdot)$ ) with noise residuals ( $\epsilon^w, \epsilon^l$ ) in noise distribution space, learning preservation-compliance balance ( $\cdot$  denotes  $F(c_p, c_i)$  and  $t$ ).

shared latent space to achieve coarse-grained preliminary visual-textual alignment essential for subsequent cross-modal fusion. This design preserves the original text-image correlation capabilities from base model while enabling synergistic cross-modal interaction.

As illustrated in Figure 5, we introduce a lightweight adaptation module comprising two key components: (1) Image Projection Module (IPM): A multilayer perceptron that maps CLIP visual features to the cross-attention dimension, eliminating the need for visual encoder fine-tuning. (2) Image Cross-Attention Module (ICAM): A direct adaptation of original text cross-attention mechanism used in SD. To formalize the interaction between these components, the following equations define their operations:

$$c_i = \text{IPM}(x_i) = \text{MLP}(\text{CLIP}(x_i)) \quad (10)$$

$$z = \text{ICAM}(Q, K^i, V^i) = \text{Softmax}\left(\frac{Q(K^i)^\top}{\sqrt{d}}\right)V^i \quad (11)$$

where  $K^i = W^k \cdot c_i$  and  $V^i = W^v \cdot c_i$ ,  $W^k$  and  $W^v$  are trainable parameters.

Crucially, while the base diffusion model remains entirely frozen, only lightweight components of IPM-ICAM (merely 1.33% of base model parameters) are updated during training. This preserves the model original generative capabilities while enabling controlled subject manipulation through the learned adapter.

#### 4.4. Direct Subject Diffusion Optimization

Building upon the aligned multimodal representations, we propose Direct Subject Diffusion (DSD) objective, the first Direct Preference Optimization adaptation for SDIG. Unlike conventional DPO that operates solely on text prompts, DSD extends to visual subjects and textual instructions, encoding user preference via supervised winning/losing image pairs. This multimodal preference modeling framework enables fine-grained supervision based on the perceived quality of generated outputs without relying on per-sample reward engineering or direct loss formulations for subjective concepts. Each training instance  $(x_p, x_i, y_0^w, y_0^l \in \mathcal{D})$  conditions generation on both textual and visual inputs, where  $y_0^w \succ y_0^l$  indicates human preference for preservation-compliance balance. To inject multimodal conditioning into the generation process, we leverage the IPM-ICAM adapter, which transforms and aligns visual and textual features into a shared representation. Specifically, the conditioning signal can be formalized as:

$$F(c_p, c_i) = \underbrace{\text{Attention}(Q, K^p, V^p)}_{\text{Text Guidance}} + \gamma \cdot \underbrace{\text{ICAM}(Q, K^i, V^i)}_{\text{Subject Anchoring}} \quad (12)$$

The text guidance term interprets the instruction semantics and encapsulates high-level editing intent. The subject anchoring term reinforces the presence and identity of the visual subject extracted



from the image. These two components are weighted by a hyperparameter  $\gamma$  to allow flexible control over the influence of the visual cue, with  $\gamma = 0$  reducing the model to standard text-to-image diffusion.

For each target pair, we apply DDIM forward diffusion to produce noisy latent variables  $(y_t^w, y_t^l)$ , along with their corresponding noise residuals  $\epsilon^w$  and  $\epsilon^l$  at timestep  $t$ . The model, parameterized by  $\theta$ , is trained to predict the original noise from each noisy latent (i.e.,  $\epsilon_\theta(y_t^w, F(c_p, c_i), t)$ ). Finally, based on Eq.(8) and Eq.(12), our proposed Direct Subject Diffusion (DSD) objective extends conventional DPO to handle the unique requirements of subject-conditioned generation:

$$L_{\text{DSD}}(\theta) = -\mathbb{E}_{(p, i, y_0^w, y_0^l) \sim \mathcal{D}, t \sim \mathcal{U}(0, T), y_t^w \sim q(y_t^w | y_0^w), y_t^l \sim q(y_t^l | y_0^l)} \log \sigma \left( -\beta T \omega(\lambda_t) \left( \underbrace{\|\epsilon^w - \epsilon_\theta(y_t^w, F(c_p, c_i), t)\|_2^2}_{\text{Preference Alignment}} - \underbrace{\|\epsilon^w - \epsilon_{\text{ref}}(y_t^w, F(c_p, c_i), t)\|_2^2}_{\text{Reference Regularization}} - \underbrace{\|\epsilon^l - \epsilon_\theta(y_t^l, F(c_p, c_i), t)\|_2^2}_{\text{Dispreference Repulsion}} + \underbrace{\|\epsilon^l - \epsilon_{\text{ref}}(y_t^l, F(c_p, c_i), t)\|_2^2}_{\text{Reference Normalization}} \right) \right) \quad (13)$$

Here  $\epsilon_\theta$  denotes the noise prediction from trainable model, while  $\epsilon_{\text{ref}}$  represents the prediction from a frozen reference model. The temperature hyperparameter  $\beta$ , number of diffusion steps  $T$ , and timestep weighting function  $\omega(\lambda_t)$  are used to scale gradients dynamically across sampling steps.

Each term in the DSD loss supports a distinct optimization role: (1) Preference Alignment encourages the model to predict noise close to the target noise of the winning image, thereby learning to reproduce the generation direction that leads to preferred outcomes. (2) Reference Regularization penalizes the model less when the frozen reference already closely matches the winning image. This ensure the model learns where improvement over the reference model is possible. (3) Dispreference Repulsion drives the model away from replicating the noise trajectory of the losing image, explicitly suppressing undesirable generation behaviors. (4) Reference Normalization preserves the baseline behavior of the reference model on dispreferred samples and allows selective suppression of undesirable patterns while retaining valid generation capabilities, just like the negative sample rectification mechanism.

Through this design, DSD integrates preference cues directly into the generative denoising process, circumventing the need for explicit per-pixel supervision or hand-crafted reward functions. Critically, since the base diffusion model remains frozen, the learning is fully captured by the lightweight adapter modules, making the optimization both efficient and stable. This setup ensures the model is steered toward generating outputs that more closely reflect human-aligned quality, while maintaining subject identity and layout fidelity as per the given instruction.

## 5. Experiments

### 5.1. Implementation Details and Evaluation

Our experimental environment utilized 2 NVIDIA V100 GPUs(32GB). Each training run consisted of 50 epochs (40,000 steps) with a batch size of 8, and a learning rate of  $1e-5$ , along with a warmup scheduler. Each epoch took approximately 35 minutes to complete. Our model is trained on C4DD, with detailed dataset construction described in Sec 4.1. In order to validate the generation capability in the open domain, we evaluate our model not only in Concept101 [Kumari et al.(2023)], but also follow the DreamBench [Ruiz et al.(2023)] for quantitative and qualitative comparison. DreamBench includes 30 subjects with 25 instructions while Concept101 includes 101 subjects with different 20 instructions for each subject. Although Custom Diffusion provided Concept101 for human preference assessment, we keep the automatic evaluation so calculate the CLIP visual similarity (CLIP-I) and DINO similarity between the generated images and the target subject images as subject alignment, and calculate the CLIP text-image similarity (CLIP-T) between the generated images and the given text instruction as text alignment.

We compare several methods for personalized image generation, including Textual Inversion [Gal et al.(2022)], DreamBooth [Ruiz et al.(2023)] and Custom Diffusion [Kumari et al.(2023)]. These methods require test-time fine-tuning on given personalized images within specific category. In addition, we compare ELITE [Wei et al.(2023)], BLIP-Diffusion [Li et al.(2023)], IP-adapter [Ye et al.(2023)], SSR-Encoder [Zhang et al.(2024)] and Subject Diffusion [Ma et al.(2024)], all of which trained on a large-scale open-domain dataset without test-time fine-tuning. All baseline methods and our proposed approach are implemented based on the same Stable Diffusion model (SD v1.5) for fair comparison.

### 5.2. Experiment Results

**Quantitative comparison.** Table 1 presents our quantitative evaluation across two benchmarks: Concept101 and DreamBench. We follow DreamBooth to generate 6 images for each text prompt provided from DreamBench or Concept101, amounting to a total 4,500 and 12,120 images for all the subjects. We report the average DINO, CLIP-I and CLIP-T scores over all pairs of real and generated images. Our comprehensive evaluation across two benchmark datasets demonstrates our method achieves superior scores on all CLIP-I and CLIP-T metrics across both test sets, outperforming all eight baseline methods by significant margins. In the DreamBench evaluation, while our approach ranks first in CLIP-I (with 0.826 score) and CLIP-T (0.314), it attains a competitive second position in DINO scoring (0.676), which still exceeds six other comparative methods and trails the leader by 3.5%. This minor variation in a single metric across one dataset does not diminish the overall dominance of the method, particularly given its consistent top-tier performance in text-alignment (CLIP-T) and image-quality (CLIP-I) metrics that are often prioritized for subject-driven generation tasks.

Critically, the experiment results on DreamBench show that our model does not merely memorize training data. Instead, it successfully handles unseen subject-command combinations, includ-

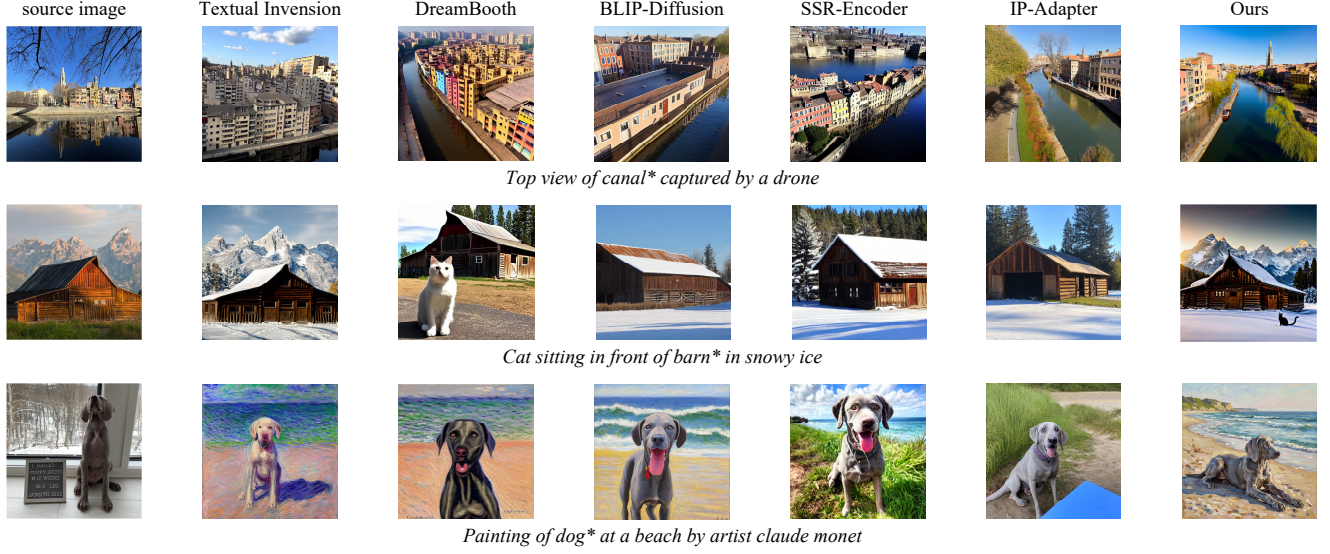


Figure 6: Quantitative Comparison between TIDE with text-driven image generation methods [Gal et al.(2022), Ruiz et al.(2023), Li et al.(2023), Zhang et al.(2024), Ye et al.(2023)]. Our model achieves significantly higher subject fidelity and prompt adherence, particularly for complex, long-form textual instruction.

Table 1: Quantitative comparisons on Concept101 and DreamBench. DreamBench results are referenced from Subject-Diffusion and SSR-Encoder. Concept101 results were tested by ourselves. All methods use SD v1.5 as base model. The best results are **bolded**, and the second-best results are underlined.

Type	Method	Concept101			DreamBench		
		CLIP-T	CLIP-I	DINO	CLIP-T	CLIP-I	DINO
Fine-tuning Based	Textual Inversion	0.280	0.786	0.670	0.255	0.780	0.569
	DreamBooth	<u>0.303</u>	0.753	0.638	0.305	0.803	0.668
	Custom Diffusion	0.274	0.789	0.658	0.287	0.788	0.653
Fine-tuning Free	ELITE	0.295	0.763	0.611	0.298	0.775	0.605
	BLIP-Diffusion	0.270	0.797	0.681	0.300	0.779	0.594
	IP-Adapter	0.271	<u>0.812</u>	<u>0.687</u>	0.274	0.809	0.608
	SSR-Encoder	0.297	0.805	0.672	<u>0.308</u>	<u>0.821</u>	0.612
	Subject-Diffusion	0.300	0.792	0.686	0.293	0.787	<b>0.711</b>
	TIDE(ours)	<b>0.304</b>	<b>0.814</b>	<b>0.690</b>	<b>0.314</b>	<b>0.826</b>	<u>0.676</u>

ing rare object categories and novel pose descriptions, achieving a 6.8% higher DINO score than the baseline model (IP-Adapter). This performance gap underscores our model’s robust generalization to unencountered scenarios, a key requirement for practical subject-driven generation.

Figure 6 presents a qualitative comparison of different SDIG methods across diverse prompts. Methods such as BLIP-Diffusion, IP-Adapter, SSR-Encoder, Textual Inversion and DreamBooth exhibit noticeable degradation in subject fidelity compared to our method. Notably, our method achieves subject preservation quality comparable to multi-image DreamBooth fine-tuning, while simultaneously maintaining superior text-alignment consistency, in contrast to the typical need for 3–5 reference images in DreamBooth.

### 5.3. Ablation Studies

**Direct Subject Diffusion Loss Ablation.** While Direct Preference Optimization loss was designed for language model alignment, we adapt it to subject-driven image generation through DSD loss, a variant that specifically addresses two domain-specific requirements: (1) precise appearance feature preservation and (2) instruction-aware subject composition. This domain adaptation unlocks nuanced control beyond conventional DPO. To further validate the design choices of DSD, we conduct controlled experiments on the C4DD dataset, varying the fusion weight  $\phi$  in Eq.(9) that governs text-visual preference balance. As shown as Figure 8, we find  $\phi = 0.7$  achieves peak performance (0.814 CLIP-I, 0.304 CLIP-T), demonstrating a 3% improvement over the training set reference images. This confirms the necessity of balanced text-

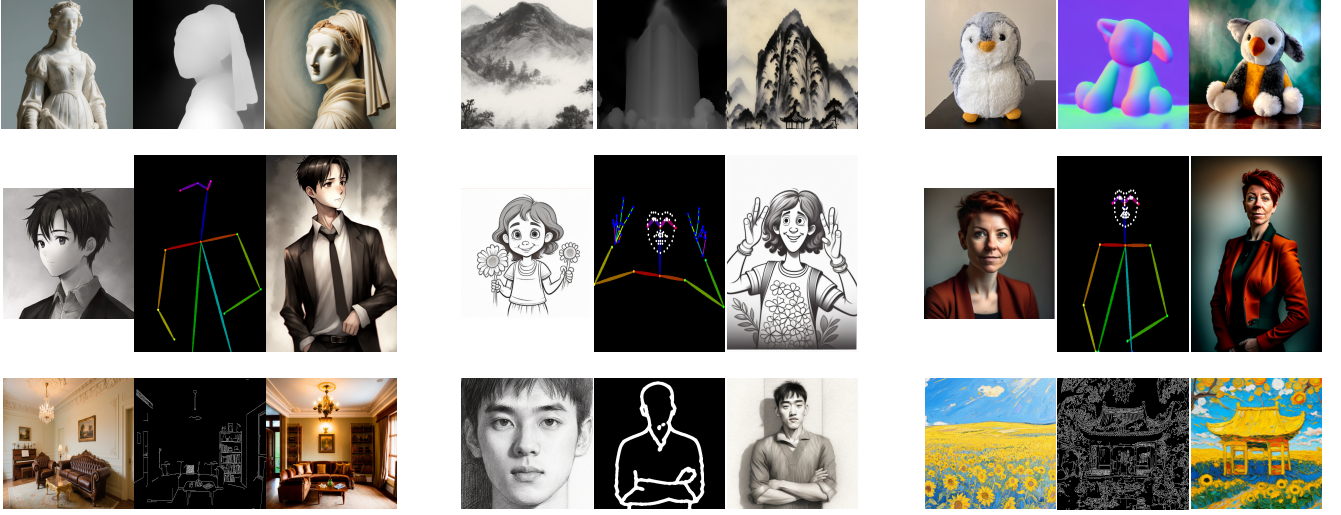


Figure 7: Visualization of model-generated images: utilizing image prompts under diverse structural conditions.

visual alignment in subject-driven tasks. Across all  $\phi$  configurations, our method demonstrates consistent improvements over the original training data, achieving an average 1.9% enhancement in the composite metric. This marginal but statistically significant gain confirms that DSD optimization effectively distills transferable knowledge beyond mere dataset replication preference-based contrastive learning. This ablation confirms the role of DSD as a domain-optimized instantiation of DPO for subject-driven image generation, where simultaneous control of subject identity and editable attributes is paramount.

Table 2: Ablation study of different components

Method	Index	Evaluation Metrics		
		CLIP-T	CLIP-I	DINO
Full Model	(a)	<b>0.314</b>	<b>0.826</b>	<b>0.676</b>
w/o training on C4DD	(b)	0.274	0.809	0.608
w/o DSD loss	(c)	0.275	0.820	0.665
w/o target supervision	(d)	0.265	0.815	0.668
w/o IPM-ICAM	(e)	0.299	0.719	0.637

**Different Components Ablation.** Table 2 presents zero-shot evaluation results on DreamBench, systematically assessing the impact of individual components in our proposed framework. Each ablation setting (b–e) exhibits quantitatively inferior performance compared to the full model (a), underscoring the critical role of each component in achieving optimal results.

Experiment (b) serves as the baseline model (IP-Adapter), trained solely on OpenImages with self-supervised reconstruction objectives. Our evaluation results (a) and (b) demonstrate that integrating our C4DD dataset significantly enhances the generative capabilities of the baseline. This confirms that the tailored dataset effectively bridges the gap between generic vision-language alignment and subject-driven image generation tasks.

The comparison between (a) and (c) isolates the contribution

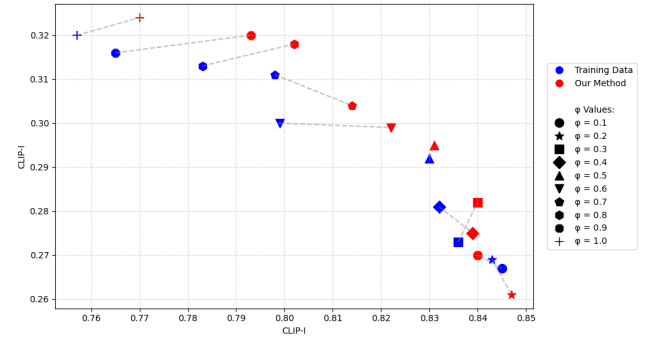


Figure 8: Ablation study on DSD impact, where data points positioned closer to the top-right corner of the plot indicate superior performance.

of the DSD loss function. The inclusion of DSD yields substantial gains across all metrics (with the CLIP-T score increasing by 3.9%, the CLIP-I increasing by 0.6%, and DINO score increasing by 1.9%). This improvement is particularly pronounced in semantic fidelity (CLIP-T), suggesting that DSD loss plays a crucial role in enabling the model to effectively capture fine-grained semantic nuances.

Experiments (a) vs. (d) highlight the importance of target supervision. Following the self-supervised reconstruction experiment setup, using the "winning" images as input images in experiment (d) leads to a 4.9% drop in the CLIP-T metric. This degradation arises because the small scale of C4DD is insufficient to support robust self-supervised learning without explicit guidance.

The results of (a) and (e) emphasize the criticality of the IPM-ICAM feature fusion mechanism. Removing this component results in a precipitous decline in CLIP-I (-10.7%), indicating a loss



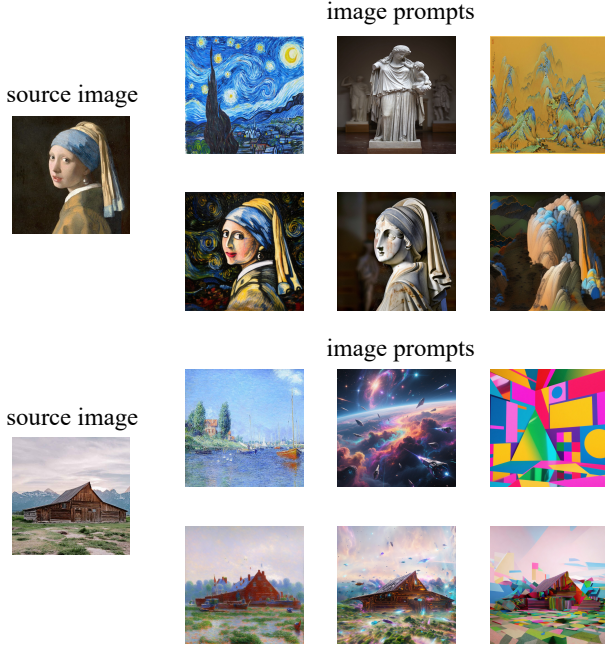


Figure 9: Visualization of image-to-image by our model.

of subject fidelity. This demonstrates that IPM-ICAM effectively aggregates multimodal features to preserve subject characteristics during generation.

#### 5.4. More Applications

Although the proposed TIDE is designed to achieve the generation with image prompts, its robust generalization capabilities allow for a broader range of applications. TIDE is not only efficient in subject-driven image generation but also compatible with existing controllable tools and text prompts. In this part, we show more results that our model can generate.

**Structural Condition.** A pivotal advantage of text-to-image diffusion models lies in their capacity for structural-conditioned generation. Crucially, the adapter architecture of TIDE preserves the native compatibility of base model with existing control mechanisms (e.g., ControlNet [Zhang et al.(2023)]), enabling multi-condition synthesis. As demonstrated in Figure 7, TIDE successfully processes diverse control modalities, including depth map, normal map, human pose skeleton, canny edge and free-form scribble. Notably, this functionality requires no additional fine-tuning and the parameter-efficient design of the adapter ensures seamless interoperability with control tools while avoiding catastrophic interference. The simultaneous satisfaction of structural constraints and subject preservation demonstrates the capability of TIDE for multi-condition generation without control-specific tuning.

**Image-to-Image Generation.** TIDE naturally extends to image-to-image style transfer by leveraging its core subject-preservation architecture. Given a content image and style reference, the framework seamlessly transfers artistic attributes (e.g., brushstrokes,

color palettes) while rigorously maintaining the structural integrity of the original subject. As illustrated in Figure 9, this enables convincing transformations across diverse media (from watercolor renditions to synthetic art styles) without distorting key subject characteristics. Honed during preference optimization, the adapter innately understands subject-style relationships, enabling it to intelligently balance stylistic adaptation with identity preservation. This capability outperforms conventional style transfer tools, which often compromise subject fidelity.

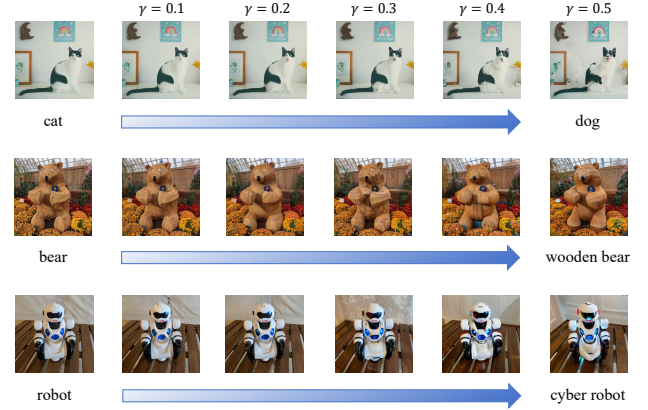


Figure 10: Text-image interpolation.

**Latent Space Interpolation.** As formalized in Eq.(12), TIDE governs cross-modal interpolation through the tunable parameter  $\gamma$ , which dynamically weights the contributions of text and image embeddings to precisely control the balance between text and image references during attribute transitions. As demonstrated in Figure 10, smooth interpolations across subject, material and style attributes are achieved within a  $\gamma$  range of 0.1 to 0.5, while maintaining exceptional background consistency and subject fidelity. This smoothness ensures artistically viable transitions without perceptual discontinuities. When  $\gamma$  exceeds 0.5, the model’s attention to visual references diminishes, causing a gradual degradation into conventional text-to-image generation as textual guidance becomes disproportionately dominant. This behavior is not a failure mode but rather an expected outcome of our training strategy, which prioritizes structural alignment through carefully calibrated  $\gamma$  values to ensure robust subject preservation while still allowing flexible attribute manipulation.

#### 6. Conclusion

TIDE establishes a new framework for subject-driven image generation by resolving the fundamental preservation-compliance trade-off through target-supervised learning and preference optimization. Our framework eliminates test-time fine-tuning via a lightweight multimodal adapter that fuses visual-textual features while preserving base model integrity. Methodologically, this represents a paradigm shift from reconstruction-based self-supervision to instruction-target aligned learning, enabling unprecedented precision in subject-instruction coordination.

Extensive validation demonstrates the superiority of TIDE in



maintaining subject fidelity ( $\uparrow$  6.8% DINO score over the baseline model) and instruction compliance ( $>$  31% CLIP-T score), with zero-shot adaptability to structural editing, image-to-image translation, and interpolation tasks. These capabilities position TIDE as a foundational tool for creative industries requiring reliable subject manipulation, from personalized advertising to educational content generation. This work bridges the gap between precise subject control and flexible instruction following, opening avenues for instruction-aware generative systems.

## 7. Limitation

Although our method enables zero-shot generation for arbitrary open-domain subjects, it still has certain limitations. The framework inherits the text comprehension constraints of CLIP, and notably, existing methods have not yet focused on addressing the fragmented or complex paragraph-length instructions which exceed typical token thresholds. Additionally, handling minority languages may trigger subject-instruction misalignment due to insufficient multilingual training data, potentially leading to hallucinated outputs in non-dominant language scenarios. In the future, we plan to integrate additional techniques to overcome these limitations while maintaining the efficiency benefits of our current paradigm.

## References

- [Achiam et al.(2023)] Josh Achiam, Steven Adler, Sandhini Agarwal, Lama Ahmad, Ilge Akkaya, Florencia Leoni Aleman, Diogo Almeida, Janko Altmenschmidt, Sam Altman, Shyamal Anadkat, et al. 2023. Gpt-4 technical report. *arXiv preprint arXiv:2303.08774* (2023). 3
- [Ahn et al.(2024)] Donghoon Ahn, Hyoungwon Cho, Jaewon Min, Wooseok Jang, Jungwoo Kim, SeonHwa Kim, Hyun Hee Park, Kyong Hwan Jin, and Seungryong Kim. 2024. Self-rectifying diffusion sampling with perturbed-attention guidance. In *European Conference on Computer Vision*. Springer, 1–17. 2
- [Avrahami et al.(2023)] Omri Avrahami, Kfir Aberman, Ohad Fried, Daniel Cohen-Or, and Dani Lischinski. 2023. Break-a-scene: Extracting multiple concepts from a single image. In *SIGGRAPH Asia 2023 Conference Papers*. 1–12. 2
- [Bai et al.(2022)] Yuntao Bai, Saurav Kadavath, Sandipan Kundu, Amanda Askell, Jackson Kernion, Andy Jones, Anna Chen, Anna Goldie, Azalia Mirhoseini, Cameron McKinnon, et al. 2022. Constitutional ai: Harmlessness from ai feedback. *arXiv preprint arXiv:2212.08073* (2022). 3
- [Chefer et al.(2024)] Hila Chefer, Oran Lang, Mor Geva, Volodymyr Polosukhin, Assaf Shocher, Michal Irani, Inbar Mosseri, and Lior Wolf. 2024. The Hidden Language of Diffusion Models. In *12th International Conference on Learning Representations, ICLR 2024*. 2
- [Dhariwal and Nichol(2021)] Prafulla Dhariwal and Alexander Nichol. 2021. Diffusion models beat gans on image synthesis. *Advances in neural information processing systems* 34 (2021), 8780–8794. 2
- [Ding et al.(2024)] Ganggui Ding, Canyu Zhao, Wen Wang, Zhen Yang, Zide Liu, Hao Chen, and Chunhua Shen. 2024. Freecustom: Tuning-free customized image generation for multi-concept composition. In *Proceedings of the IEEE/CVF Conference on Computer Vision and Pattern Recognition*. 9089–9098. 4
- [Dong et al.(2023)] Guanting Dong, Hongyi Yuan, Keming Lu, Chengpeng Li, Mingfeng Xue, Dayiheng Liu, Wei Wang, Zheng Yuan, Chang Zhou, and Jingren Zhou. 2023. How abilities in large language models are affected by supervised fine-tuning data composition. *arXiv preprint arXiv:2310.05492* (2023). 3
- [Dubois et al.(2023)] Yann Dubois, Chen Xuechen Li, Rohan Taori, Tianyi Zhang, Ishaan Gulrajani, Jimmy Ba, Carlos Guestrin, Percy S Liang, and Tatsunori B Hashimoto. 2023. AlpacaFarm: A simulation framework for methods that learn from human feedback. *Advances in Neural Information Processing Systems* 36 (2023), 30039–30069. 3
- [Gal et al.(2022)] Rinon Gal, Yuval Alaluf, Yuval Atzmon, Or Patashnik, Amit H Bermano, Gal Chechik, and Daniel Cohen-Or. 2022. An image is worth one word: Personalizing text-to-image generation using textual inversion. *arXiv preprint arXiv:2208.01618* (2022). 2, 3, 7, 8
- [Gal et al.(2023)] Rinon Gal, Moab Arar, Yuval Atzmon, Amit H Bermano, Gal Chechik, and Daniel Cohen-Or. 2023. Encoder-based domain tuning for fast personalization of text-to-image models. *ACM Transactions on Graphics (TOG)* 42, 4 (2023), 1–13. 3
- [Han et al.(2023)] Ligong Han, Yinxiao Li, Han Zhang, Peyman Milanfar, Dimitris Metaxas, and Feng Yang. 2023. Svdif: Compact parameter space for diffusion fine-tuning. In *Proceedings of the IEEE/CVF International Conference on Computer Vision*. 7323–7334. 3
- [Hyung et al.(2024)] Junha Hyung, Jaeyo Shin, and Jaegul Choo. 2024. Magicapture: High-resolution multi-concept portrait customization. In *Proceedings of the AAAI Conference on Artificial Intelligence*, Vol. 38. 2445–2453. 2, 3
- [Imrey(2005)] Peter B Imrey. 2005. Bradley-Terry Model. *Encyclopedia of Biostatistics* 1 (2005). 4
- [Kingma et al.(2021)] Diederik Kingma, Tim Salimans, Ben Poole, and Jonathan Ho. 2021. Variational diffusion models. *Advances in neural information processing systems* 34 (2021), 21696–21707. 4
- [Krishnaiah et al.(2024)] N Krishnaiah, Vastrala Vaishnavi, Ch Thanmai, D Pranathi, G Sunaina, K Gayathri Bhavya, and M Aditi. 2024. Harmonizing Offline Reinforcement Learning with Language Models Analysis of Human Responses. *learning* 24, 2 (2024). 3
- [Kumari et al.(2023)] Nupur Kumari, Bingliang Zhang, Richard Zhang, Eli Shechtman, and Jun-Yan Zhu. 2023. Multi-concept customization of text-to-image diffusion. In *Proceedings of the IEEE/CVF conference on computer vision and pattern recognition*. 1931–1941. 2, 3, 5, 7
- [Kuznetsova et al.(2020)] Alina Kuznetsova, Hassan Rom, Neil Alldrin, Jasper Uijlings, Ivan Krasin, Jordi Pont-Tuset, Shahab Kamali, Stefan Popov, Matteo Mallocci, Alexander Kolesnikov, et al. 2020. The open images dataset v4: Unified image classification, object detection, and visual relationship detection at scale. *International journal of computer vision* 128, 7 (2020), 1956–1981. 3, 4
- [Li et al.(2023)] Dongxu Li, Junnan Li, and Steven Hoi. 2023. Blip-diffusion: Pre-trained subject representation for controllable text-to-image generation and editing. *Advances in Neural Information Processing Systems* 36 (2023), 30146–30166. 2, 3, 4, 7, 8
- [Lin et al.(2024)] Zhihang Lin, Mingbao Lin, Meng Zhao, and Rongrong Ji. 2024. Accdiffusion: An accurate method for higher-resolution image generation. In *European Conference on Computer Vision*. Springer, 38–53. 3
- [Liu et al.(2023a)] Zhiheng Liu, Ruili Feng, Kai Zhu, Yifei Zhang, Kecheng Zheng, Yu Liu, Deli Zhao, Jingren Zhou, and Yang Cao. 2023a. Cones: Concept neurons in diffusion models for customized generation. *arXiv preprint arXiv:2303.05125* (2023). 3
- [Liu et al.(2023b)] Zhiheng Liu, Yifei Zhang, Shen Yujun, Zheng Kecheng, Kai Zhu, Ruili Feng, Liu Yu, Deli Zhao, Jingren Zhou, and Cao Yang. 2023b. Cones 2: Customizable Image Synthesis with Multiple Subjects. *arXiv preprint arXiv:2305.19327* (2023). 3
- [Ma et al.(2024)] Jian Ma, Junhao Liang, Chen Chen, and Haonan Lu. 2024. Subject-diffusion: Open domain personalized text-to-image generation without test-time fine-tuning. In *ACM SIGGRAPH 2024 Conference Papers*. 1–12. 2, 3, 4, 7
- [Ma et al.(2023)] Yiyang Ma, Huan Yang, Wenjing Wang, Jianlong Fu, and Jiaying Liu. 2023. Unified multi-modal latent diffusion for joint subject and text conditional image generation. *arXiv preprint arXiv:2303.09319* (2023). 3

- [Mnih et al.(2016)] Volodymyr Mnih, Adria Puigdomenech Badia, Mehdi Mirza, Alex Graves, Timothy Lillicrap, Tim Harley, David Silver, and Koray Kavukcuoglu. 2016. Asynchronous methods for deep reinforcement learning. In *International conference on machine learning*. Pmlr, 1928–1937. 3
- [Podell et al.(2023)] Dustin Podell, Zion English, Kyle Lacey, Andreas Blattmann, Tim Dockhorn, Jonas Müller, Joe Penna, and Robin Rombach. 2023. Sdxl: Improving latent diffusion models for high-resolution image synthesis. *arXiv preprint arXiv:2307.01952* (2023). 3
- [Rafailov et al.(2023)] Rafael Rafailov, Archit Sharma, Eric Mitchell, Christopher D Manning, Stefano Ermon, and Chelsea Finn. 2023. Direct preference optimization: Your language model is secretly a reward model. *Advances in Neural Information Processing Systems* 36 (2023), 53728–53741. 3, 4
- [Raffel et al.(2020)] Colin Raffel, Noam Shazeer, Adam Roberts, Katherine Lee, Sharan Narang, Michael Matena, Yanqi Zhou, Wei Li, and Peter J Liu. 2020. Exploring the limits of transfer learning with a unified text-to-text transformer. *Journal of machine learning research* 21, 140 (2020), 1–67. 3
- [Ramesh et al.(2022)] Aditya Ramesh, Prafulla Dhariwal, Alex Nichol, Casey Chu, and Mark Chen. 2022. Hierarchical text-conditional image generation with clip latents. *arXiv preprint arXiv:2204.06125* 1, 2 (2022), 3. 3
- [Ramesh et al.(2021)] Aditya Ramesh, Mikhail Pavlov, Gabriel Goh, Scott Gray, Chelsea Voss, Alec Radford, Mark Chen, and Ilya Sutskever. 2021. Zero-shot text-to-image generation. In *International conference on machine learning*. Pmlr, 8821–8831. 3
- [Rombach et al.(2022)] Robin Rombach, Andreas Blattmann, Dominik Lorenz, Patrick Esser, and Björn Ommer. 2022. High-resolution image synthesis with latent diffusion models. In *Proceedings of the IEEE/CVF conference on computer vision and pattern recognition*. 10684–10695. 2, 3
- [Ruiz et al.(2023)] Nataniel Ruiz, Yuanzhen Li, Varun Jampani, Yael Pritch, Michael Rubinstein, and Kfir Aberman. 2023. Dreambooth: Fine tuning text-to-image diffusion models for subject-driven generation. In *Proceedings of the IEEE/CVF conference on computer vision and pattern recognition*. 22500–22510. 2, 3, 7, 8
- [Saharia et al.(2022)] Chitwan Saharia, William Chan, Saurabh Saxena, Lala Li, Jay Whang, Emily L Denton, Kamyar Ghasemipour, Raphael Gontijo Lopes, Burcu Karagol Ayan, Tim Salimans, et al. 2022. Photorealistic text-to-image diffusion models with deep language understanding. *Advances in neural information processing systems* 35 (2022), 36479–36494. 3
- [Schuhmann et al.(2022)] Christoph Schuhmann, Romain Beaumont, Richard Vencu, Cade Gordon, Ross Wightman, Mehdi Cherti, Theo Coombes, Aarush Katta, Clayton Mullis, Mitchell Wortsman, et al. 2022. Laion-5b: An open large-scale dataset for training next generation image-text models. *Advances in neural information processing systems* 35 (2022), 25278–25294. 4
- [Schuhmann et al.(2021)] Christoph Schuhmann, Richard Vencu, Romain Beaumont, Robert Kaczmarczyk, Clayton Mullis, Aarush Katta, Theo Coombes, Jenia Jitsev, and Aran Komatsuzaki. 2021. Laion-400m: Open dataset of clip-filtered 400 million image-text pairs. *arXiv preprint arXiv:2111.02114* (2021). 3
- [Shi et al.(2024)] Jing Shi, Wei Xiong, Zhe Lin, and Hyun Joon Jung. 2024. Instantbooth: Personalized text-to-image generation without test-time finetuning. In *Proceedings of the IEEE/CVF conference on computer vision and pattern recognition*. 8543–8552. 3
- [Skalse et al.(2022)] Joar Skalse, Nikolaus Howe, Dmitrii Krasheninikov, and David Krueger. 2022. Defining and characterizing reward gaming. *Advances in Neural Information Processing Systems* 35 (2022), 9460–9471. 3
- [Song et al.(2020)] Jiaming Song, Chenlin Meng, and Stefano Ermon. 2020. Denoising Diffusion Implicit Models. In *International Conference on Learning Representations*. 4
- [Tewel et al.(2023)] Yoad Tewel, Rinon Gal, Gal Chechik, and Yuval Atzmon. 2023. Key-locked rank one editing for text-to-image personalization. In *ACM SIGGRAPH 2023 conference proceedings*. 1–11. 3
- [Wallace et al.(2024)] Bram Wallace, Meihua Dang, Rafael Rafailov, Linqi Zhou, Aaron Lou, Senthil Purushwalkam, Stefano Ermon, Caiming Xiong, Shafiq Joty, and Nikhil Naik. 2024. Diffusion model alignment using direct preference optimization. In *Proceedings of the IEEE/CVF Conference on Computer Vision and Pattern Recognition*. 8228–8238. 3, 4
- [Wang et al.(2024)] Yibin Wang, Weizhong Zhang, Jianwei Zheng, and Cheng Jin. 2024. High-fidelity person-centric subject-to-image synthesis. In *Proceedings of the IEEE/CVF Conference on Computer Vision and Pattern Recognition*. 7675–7684. 3
- [Wei et al.(2023)] Yuxiang Wei, Yabo Zhang, Zhilong Ji, Jinfeng Bai, Lei Zhang, and Wangmeng Zuo. 2023. Elite: Encoding visual concepts into textual embeddings for customized text-to-image generation. In *Proceedings of the IEEE/CVF International Conference on Computer Vision*. 15943–15953. 3, 7
- [Xiao et al.(2024)] Guangxuan Xiao, Tianwei Yin, William T Freeman, Frédo Durand, and Song Han. 2024. Fastcomposer: Tuning-free multi-subject image generation with localized attention. *International Journal of Computer Vision* (2024), 1–20. 3
- [Ye et al.(2023)] Hu Ye, Jun Zhang, Sibao Liu, Xiao Han, and Wei Yang. 2023. Ip-adapter: Text compatible image prompt adapter for text-to-image diffusion models. *arXiv preprint arXiv:2308.06721* (2023). 3, 4, 7, 8
- [Ye et al.(2024)] Qinghao Ye, Haiyang Xu, Jiabo Ye, Ming Yan, Anwen Hu, Haowei Liu, Qi Qian, Ji Zhang, and Fei Huang. 2024. mplug-owl2: Revolutionizing multi-modal large language model with modality collaboration. In *Proceedings of the IEEE/CVF conference on computer vision and pattern recognition*. 13040–13051. 3
- [Zhang et al.(2023)] Lvmin Zhang, Anyi Rao, and Maneesh Agrawala. 2023. Adding conditional control to text-to-image diffusion models. In *Proceedings of the IEEE/CVF international conference on computer vision*. 3836–3847. 10
- [Zhang et al.(2024)] Yuxuan Zhang, Yiren Song, Jiaming Liu, Rui Wang, Jinpeng Yu, Hao Tang, Huaxia Li, Xu Tang, Yao Hu, Han Pan, et al. 2024. Ssr-encoder: Encoding selective subject representation for subject-driven generation. In *Proceedings of the IEEE/CVF Conference on Computer Vision and Pattern Recognition*. 8069–8078. 2, 3, 4, 7, 8